GIS Odyssey Journal

2026 • Volume 6 • Number 2

https://doi.org/10.57599/gisoj.2026.6.2.185

Samet Doğan[1], Oktay Aksu[2], Selim Taşkaya[3], Mustafa Kurt[4], Agne Karlıkanovaite-Balikci[5]

OBTAINING AND EVALUATION OF LAND SURFACE TEMPERATURE USING CLOUD-BASED APPLICATIONS: THE CASE OF ANKARA PROVINCE

Abstract: Rapid urban expansion, characterized by high land surface temperatures (LST) in urban areas, has led to environmental and health concerns along with increased energy consumption. Recent advances in remote sensing have facilitated the investigation of spatiotemporal LST patterns and their relationships with factors such as vegetation, built-up land, and soil moisture. However, a limited number of studies investigate whether these relationships differ between urban and rural areas. Leveraging the power of cloud computing resources such as Google Earth Engine (GEE) and Microsoft Azure, researchers can now examine these issues on a larger scale and over a longer period. Focusing on Ankara, the capital city known for its recent urban growth, we specifically calculated the annual average and seasonal average LST at the grid level, performed urban-rural slope analysis, examined the relationship between LST and vegetation and built-up land in urban and rural areas separately, and analyzed how LST relates to land cover types in Ankara. Using GEE for geographic spatial analysis, the study sheds light on critical issues such as the relationship between LST and various land cover types. By providing valuable insights into seasonal LST variations in various areas, the study investigates how LST relates to land characteristics in urban and rural areas and aims to assist in sustainable urban planning.

Keywords: LST, GEE, Ankara, Urban/Rural Surface Temperature, NDVI, NDBI

Received: 14 April 2026; accepted: 13 July 2026; revised: 31 August 2026

[1] Kastamonu University, Department of Architecture and Urban Planning, Kastamonu, Türkiye, ORCID ID: http://orcid.org/0000-0002-3103-1593, email: sametdogan@kastamonu.edu.tr, corresponding author
[2] Istanbul Okan University, Engineering and Natural Science Faculty, İstanbul, Türkiye, ORCID ID: http://orcid.org/0000-0001-5584-6079, email: oktay.aksu@okan.edu.tr
[3] Artvin Çoruh University, Department of Architecture and Urban Planning, Artvin, Türkiye, ORCID ID: http://orcid.org/0000-0002-4290-3684, email: selim_taskaya@artvin.edu.tr
[4] Istanbul Okan University, Engineering and Natural Science Faculty, İstanbul, Türkiye, ORCID ID: http://orcid.org/0000-0001-8470-2832, email: mustafa.kurt@okan.edu.tr
[5] Istanbul Okan University, Department of Civil Engineering, İstanbul, Türkiye, ORCID ID: http://orcid.org/0000-0002-2290-5818, email: agne.karlikanovaite@okan.edu.tr

Introduction

Rapid urban growth, driven by rising populations and densities worldwide, has significantly impacted the environment (Sonet et al., 2025; Bag et al., 2024). For example, air pollution, humidity, and land surface temperature have all gone up in cities (Mwangi et al., 2018). Urbanization is the primary factor contributing to the rise in global land surface temperature (LST), chiefly due to the substitution of natural landscapes with artificial ones. This causes urban areas to be hotter than nearby rural areas, changes in microclimates, and a higher chance of getting sick from the heat (Qian et al., 2025). It is crucial to comprehend the complex relationship between urban development and LST to mitigate the environmental impacts of urbanization (Ullah et al., 2025). Ankara's cities have been experiencing rapid growth over the last few years, with significant expansion in population, industry, and infrastructure (Bag et al., 2024). The 2010 census showed that the capital had 4.7 million people. By 2022, that number will have grown to 5.7 million (TSI, 2023). The capital's land cover and land use (LC/LU) patterns have undergone significant changes due to rapid urbanization (Islam et al., 2025). Many natural areas have been replaced by built-up areas, roads, and other surfaces that don't allow water to pass through (Golder et al., 2025). The increase in concrete structures, buildings, and impervious surfaces has been shown to store heat better than other natural surfaces (Amani et al., 2025). Ankara is growing quickly as a city, but it also has a wide range of landscapes, including forests, lakes, rivers, meadows, and humid continental zones with cold winters and hot summers. The different types of land cover (LC) and climates make it possible to study how urban growth affects land surface temperature in different settings.

A thorough comprehension of LST across spatial and temporal dimensions is essential for elucidating the environmental consequences of urban expansion and formulating sustainable development strategies (Sattar et al., 2025). Remote sensing techniques have been extensively employed to examine the correlation between urban surfaces and the thermal environment, with the objective of elucidating the effects of urban expansion on land surface temperature and pinpointing significant factors (Rahman et al., 2025). The main goals of this study are to look at the annual and seasonal spatial patterns of land surface temperature over the last ten years of urbanization in Ankara, to summarize the overall trend, and to look at the relationship between LST and different factors, such as vegetation, built-up land, distance from urban areas, and different types of land cover. The findings of this study furnish essential insights for urban planners, decision-makers, and policymakers in the domain, enabling them to guide future urban planning and management strategies in Ankara.

As countries become more urbanized, plants and trees are lost, which can make the air in cities hotter near the center (Basu et al., 2025). Changes in atmospheric pressure (A/C) and the increasing urbanization of populations are causing many ecological problems around the world. These include air pollution, adverse weather conditions, greenhouse gas emissions, and the conflict between urban development and environmental sustainability. As cities get taller, these problems are becoming more common. To come up with effective solutions, we need a lot of information. Ayanlade et al. (2021). Sarif et al. (2020) and Cao et al. (2008) utilized Landsat ETM+ and Landsat TM imagery, which offer thermal infrared and multispectral images, facilitating the examination of temporal changes over multiple decades. This makes it possible to look at changes in land cover and surface temperatures. Recent advancements also include deep learning-based segmentation algorithms for more accurate LULC mapping, even in heterogeneous environments (Sür et al., 2025).

Landsat images are thought to have a spatial resolution of 30 meters, so they might not be able to show the small details of impervious surfaces or temperature changes in smaller cities (Pleniou & Koutsias, 2025). These satellites can only see changes over time because they only fly over an area every 16 days. Ayanlade et al. (2021) emphasize the significance of examining variations in land surface temperature (LST) across ecoregions, alongside population growth, urban planning, and heat mitigation strategies. They offer important insights into the determinants influencing land surface temperature (LST) in urban settings. Scientists employ various methods to examine how temperature changes across different types of land cover and areas with hard surfaces (Sür et al., 2025).

Wang & Upreti (2019) used the WRF model to run simulations in Phoenix, Las Vegas, and Denver. They demonstrated that changes in land cover can alter the climate in a region, with common patterns of rising temperatures at night and falling temperatures during the day. Dissanayake (2020) underscored that urbanization can adversely affect the environment and economy by elevating LST, particularly in developing nations.

Li et al. (2013) observed that high-resolution imagery provides a more precise analysis of small green spaces, whereas lower resolutions may underestimate the extent and effects of green space. All studies identified an inverse correlation between green space ratio and land surface temperature (LST), although the strength of this correlation varies based on the data employed.

Ravanelli et al. (2018) demonstrate that the Google Earth Engine platform, a novel approach to Earth observation, facilitates easier data management and processing. A study investigating the correlation between alterations in land cover and recorded land surface temperature (LST) trends across six metropolitan regions over two decades introduced an innovative approach for the ratio parameter for each region (Ratio Matrix). Using more than one spectral band can make land cover classification more efficient.

Sarif et al. (2020) utilized Landsat data to delineate land use and land cover (LU/LC). They examined the impact of land use and land cover on the surface urban heat island (SUH) phenomenon by categorizing land cover into four groups: agriculture, vegetation, wasteland, and impervious surface. They showed how different types of urban land cover and changes affect SUH density, as well as how the size of buffers around urban areas affects the SUH assessment. The study suggests that examining enduring urban hotspots should prioritize identifying suitable hotspots over regions with analogous site conditions, rather than focusing on locating hotter zones within a limited area with varied urban land covers.

Materials and methods

Theoretical framework and scope. Urbanization, industrialization, and population growth have emerged as significant catalysts of global environmental change (Saxena, 2025). The natural environment is changing, and climate systems are being put under stress because more buildings are being built, especially in big cities (UN-Habitat, 2020). In the last few decades, Ankara, the capital of Türkiye, has experienced rapid growth, and as a result, it has begun to feel the effects of global climate change on a local level. This article analyzes the relationship between urbanization and climate change in the context of Ankara.

This research utilizes a qualitative methodology. The data sources comprise institutional reports from the Turkish State Meteorological Service (MGM), the Turkish Statistical Institute (TSI), and the National Oceanic and Atmospheric Administration (NOAA), in addition to an international literature review. The climatic data from Ankara were examined concerning temporal change trends. MGM (2022) says that the average temperature in Ankara has been rising every year since the 1990s. The summer temperatures of 2020, 2021, and 2022 are much higher than the average for those years. NOAA's reports on global warming say that Ankara's temperature is rising by about 0.2°C per decade (NOAA, 2023). During the same time, the number of people living in Ankara grew from about 2 million in 1980 to more than 5.7 million in 2022 (TSI, 2023). As more people move to cities, the temperature differences in the city become more noticeable, and the air quality gets worse. The loss of green spaces also puts more stress on water resources and makes it harder to adapt to climate change.

The results show that urbanization in Ankara has climate effects that go beyond just changing the city's look; they also put the long-term use of natural resources at risk. Problems like rising temperatures, dirty air, and running out of water have significant social effects because they disproportionately harm people who are already vulnerable. In this situation, Ankara's urban policies need to be changed to focus on adapting to climate change (IPCC, 2021). Climate change and urbanization in Ankara are two factors that reinforce each other. The urban heat island effect worsens as more buildings are constructed and more people move in, making the effects of climate change more apparent. Because of this, Ankara should put sustainable urban planning, investments in green infrastructure, and strategies for adapting to climate change at the top of its list of priorities.

The rise in built-up land affected Ankara just like it did the rest of the world. This study thus creates a heat map that shows the temperature pattern and the growth of the population that goes along with it. The goal of this study is to fully describe the patterns of land surface temperature in Ankara during the study period and to learn more about how they affect Ankara.

Methodology. The methodology employed in this study encompasses satellite data collection, band selection, Land Surface Temperature (LST) map generation, NDVI/NDBI map compilation, and correlation analyses. The following workflow diagrams show how I plan to reach the goals of my project (Fig. 1). For this study, GEE (Google Earth Engine) was utilized to obtain LST, rural and urban LST, and NDVI, and subsequently to determine the values for urban heat density and NDBI. The maps were exported from GEE and then set up in ArcGIS Pro (ESRI, 2024; Gorelick et al., 2017).

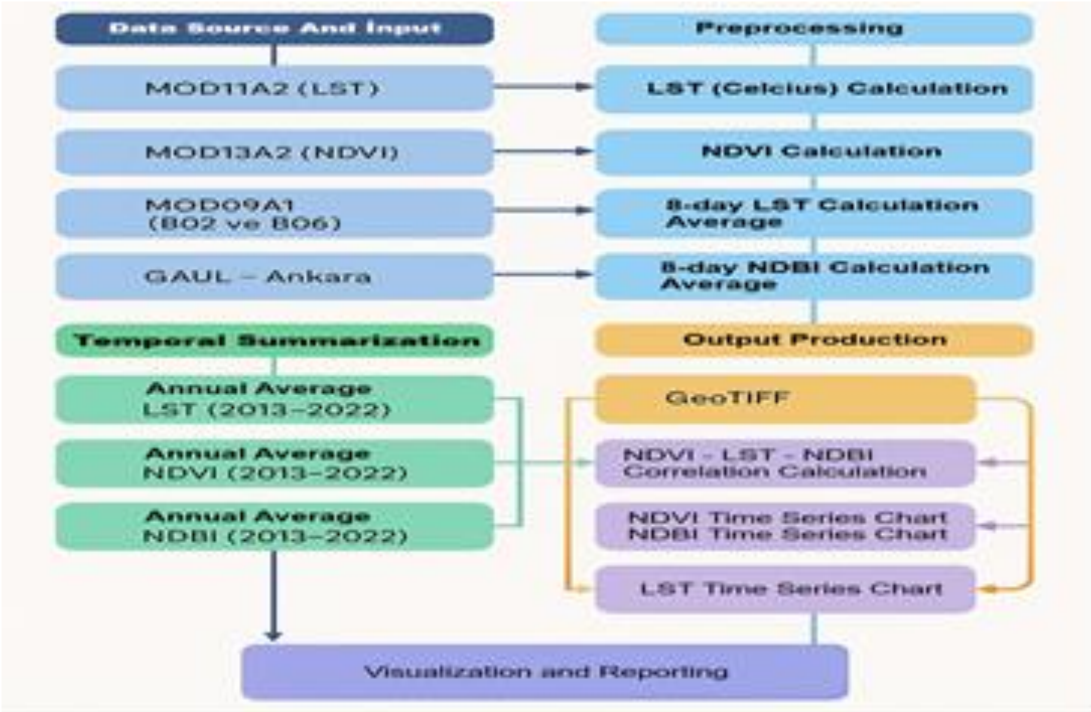

Fig. 1. Method used in the study and workflow diagram
Source: own compilation

In Fig 1., surface temperature is observed to be higher in areas with sparse vegetation and high levels of urbanization. Therefore, there is an increasing-decreasing or decreasing-increasing hierarchy between LST and NDVI.

LST Monitoring Over the Last Decade. The steps in this study were used to get LST data from the MOD11A2.061 Terra Land Surface Temperature and Emissivity 8-Day Global dataset. The LST_Day_1km band had a spatial resolution of 1 km. The GEE platform now has the MOD11A2.061 dataset as a collection of images (Rakuasa et al., 2023). After that, region and time range filters were used to reduce the number of images. The administrative border of Ankara province was used to filter the image collection for this study. The date range is from 2013 to 2022.

Method. The LST_Day_1km band had a spatial resolution of 1 km. The raw Digital Number (DN) values obtained from the MOD11A2 product were converted to Land Surface Temperature in degrees Celsius (°C) using the MODIS scale factor of 0.02 and the following conversion formula:

$$\text{LST}\ (°\text{C}) = (\text{DN} \times 0.02) - 273.15 \quad (1)$$

This conversion ensures that all subsequent LST analyses, mapping, and statistical computations are performed with physical temperature values in degrees Celsius.

We determined the annual average LST value for each pixel in the image collection of interest (Shi & Xian, 2025). A map showed the average LST image in relation to the administrative border of the Ankara province. The LST was put through a time-series analysis. For each of the years 2013, 2019, and 2022, 46 pictures were gathered and put on a list. Each element was treated like a 12-band picture of a certain date. To visualize the annual average LST and NDVI distribution, maps representing the beginning (2013), middle (2019), and end (2022) of the study period were presented. This selection was made to provide a comprehensive overview of the decadal change trends.

Time series trend analysis and trends of annual index changes are modeled using linear regression (2).

$$Y_t = \beta_0 + \beta_1 \cdot t + \epsilon_t \tag{2}$$

Here:

Y_t : LST, NDVI or NDBI value,

t : Time index (2013=0, 2014=1, ..., 2022=9),

β_1 : Annual change slope ($\beta_1 > 0$ increase, $\beta_1 < 0$ decrease

We used a t-test (α=0.05) to find out how important the slope was, and we used Sen's slope (Sen, 1968) to report the trend magnitude. This technique is extensively recognized in climatological trend analyses (IPCC, 2021).

NDVI (Normalized Difference Vegetation Index) was calculated as:

$$NDVI = \frac{(NIR - RED)}{(NIR + RED)} \tag{3}$$

where:

NIR = reflectance in the near-infrared band,

RED = reflectance in the red band.

NDVI values range from -1 to +1, with higher values indicating denser vegetation cover.

The magnitude of monotonic trends was quantified using Sen's slope estimator:

$$Q_i = \frac{(x_i - x_k)}{(j + k)} \tag{4}$$

For all (3) $j > k$,

where:

x_i and x_k are observations at times j and k,

Q_i is an individual slope estimate.

The overall Sen's slope (Q) is the median of all calculated Q_i values:

$$Q_i = median(Q_i) \tag{5}$$

A positive Q indicates an increasing trend, whereas a negative Q indicates a decreasing trend.

Study area. Ankara province is in the Central Anatolia Region of Türkiye. It is bordered by Çankırı and Bolu to the north, Kırıkkale and Kırşehir to the east, Aksaray and Konya to the south, and Eskişehir to the west. In Fig 2., Ankara is at about 32° 27' East longitude and 39° 52' North latitude. It covers an area of 25,615 km^2. About 40% of this area is made up of forests and farmland. The province has the usual features of a steppe climate and a wide range of plants. With about 5.8 million people, Ankara is the second most populous province in Türkiye (TSI, 2024). Its urban population has been growing quickly in recent years due to factors such as education, job opportunities, and improved health. Ankara is the capital of Türkiye and is known for its rich cultural and historical heritage. This is where important buildings like Anıtkabir, the Turkish Grand National Assembly, and several museums are located. Çankaya, Keçiören, and Yenimahalle are three of Ankara's biggest neighborhoods. In the past few years, people from different parts of the world have moved to Ankara, just like they have to other big cities. People from the Black Sea, Southeastern, and Eastern Anatolia areas have added to the province's population. Ankara's status as Türkiye's capital and the job and education opportunities it offers are two of the main reasons why its population is growing (Karakavak & Kadılar, 2025).

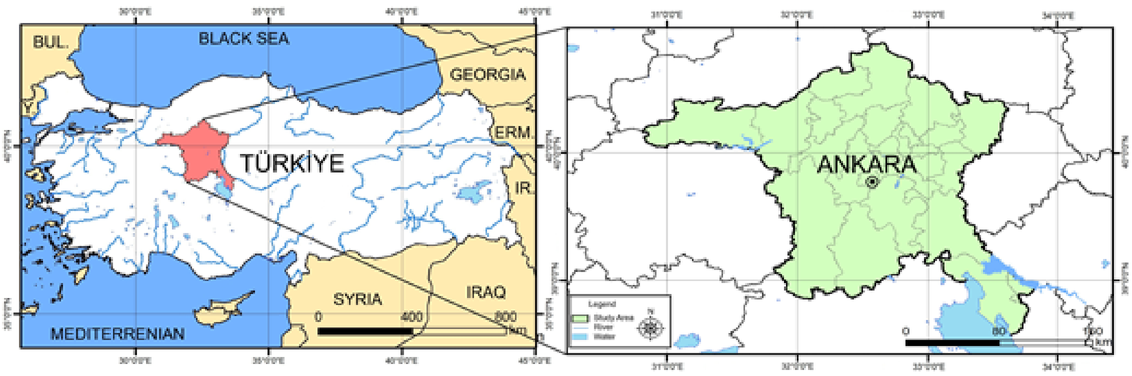

Fig. 2. Location map of study area
Source: own compilation

Results

Data. The research employed MODIS (Moderate Resolution Imaging Spectroradiometer) satellite data to examine environmental variables, including land surface temperature (LST), vegetation, and surface spectral reflectance from 2013 to 2022. The study utilized MODIS data products MOD11A2, MOD13A2, and MOD09A1, sourced from the GEE data cloud (Didan, 2015; Vermote, 2015; Wan et al., 2015).

The MOD11A2 V6.1 product gives you data on the average land surface temperature over an area of about 1200 × 1200 km for eight days. To get the temperature for each pixel, the values from the MOD11A1 product for the same 8-day period are averaged. This period for compiling data is twice as long as the entire ground monitoring period for the Terra and Aqua platforms (Gaikwad & Israr, 2025). The MOD11A2 V6.1 product features daytime and nighttime LST bands, quality control (QC) layers, and bands 31 and 32, which are utilized to determine the surface temperature.

The MOD13A2 V6.1 product gives you two 16-day composites of vegetation indices: the Normalized Difference Vegetation Index (NDVI) and the Enhanced Vegetation Index (EVI). NDVI is better for long-term studies where consistency is important, while EVI gives more accurate results in places with a lot of biomass. The best pixel for this product is chosen based on factors such as low cloud cover, a narrow angle of view, and high NDVI/EVI values (Sari et al., 2024). The study exclusively utilized NDVI data, regarded as the principal parameter for analyzing the spatial and temporal patterns of vegetation.

In Table 1., the MOD09A1 V6.1 product provides surface reflectance data from bands 1–7 of the MODIS Terra sensor for an 8-day period. The data is at a spatial resolution of 500 meters. These data, which have been corrected for atmospheric effects like gases, aerosols, and Rayleigh scattering, give reliable reflectance values in spectral analyses (Gaikwad & Israr, 2025). The dataset has four observation bands, seven reflectance bands, and a layer for quality control. In particular, Bands 2 (841–876 nm) and 6 (1628–1652 nm) were used to figure out the Urban Area Index (NDBI).

Table 1. Data sources information

Data Set	Account	Spatial resolution	Temporal resolution	Purpose of Use	Source / Platform
MOD11A2 V6.1	LST, 8 daily averages	~1 km	8 days	LST analysis	MODIS / NASA
MOD13A2 V6.1	NDVI and EVI products (vegetation indices)	~1 km	16 days	Vegetation analysis with NDVI	MODIS / NASA
MOD09A1 V6.1	Surface spectral reflectance (atmospherically corrected)	500 m	8 days	NDBI calculation (B06 B02)	MODIS / NASA
FAO/GAUL/2015	Ankara province borders (administrative geographic boundary data)	Vector (boundary)	Still	Limitation of the work area	FAO / GEE

Source: own compilation

Ravanelli et al. (2018) demonstrate that the Google Earth Engine platform reduces the complexity of data management and data processing in a modern world observation concept. In a study examining the relationship between land cover changes and observed land surface temperature (LST) trends in six metropolitan areas over a 20-year period, they introduced a novel method (Ratio Matrix) for the ratio parameter for each area. Land cover classification can be made effective using multiple spectral bands.

Sarif et al. (2020) used Landsat data to characterize land use/land cover (LU/LC) and analyzed the impact of land use and land cover on the surface urban heat island (UHI) phenomenon by classifying land cover as agriculture, vegetation, barren land, and impermeable surface. They revealed how different urban land cover types and changes affect UHI density and how the scope of buffers around urban areas affects UHI assessment. The study suggests that the analysis of persistent urban hotspots should prioritize identifying appropriately hotspots in persistent urban areas surrounded by comparable site conditions, rather than focusing on finding hotspots from a small surrounding area with diverse urban land cover.

In Fig. 3., Ankara from 2013 to 2022, maps show how the annual mean LST, summer mean LST (June, July, and August), and winter mean LST (December, January, February, March, and April) are spread out. The figure shows that 2019 had the lowest mean LST value, but it increased slightly in 2022. In 2014, the average LST in Ankara was at its highest point. As cities grow, LST values have gone up. LST values change with the seasons. In the summer, LST is higher than in the winter. In 2015, 2016, 2017, and 2019, LST went down in the summer. In 2014, 2020, and 2022, the value increased.

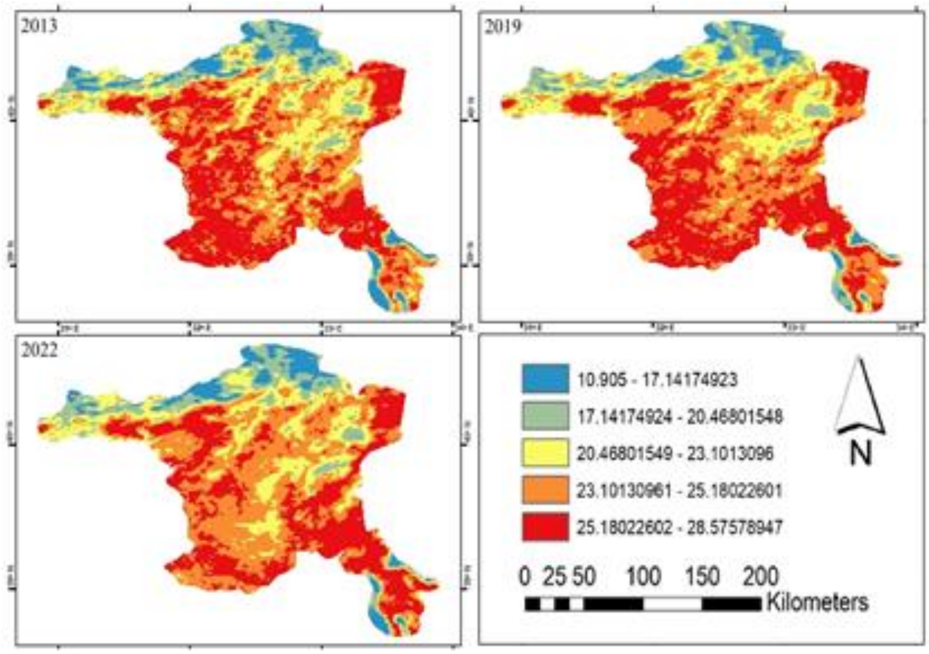

Fig. 3. Map showing the annual average Land Surface Temperature (LST) across Ankara between 2013 and 2022
Source: own compilation

The graphs show that the highest LST value occurred in the summer. This means that LST changes with the seasons. The graphs that show LST over time from 2013 to 2022 show that LST was highest in the summer of 2014 and then decreased slightly in 2022. The graphs show that LST is higher in cities and towns (where there is a lot of urban infrastructure) than in rural areas.

NDVI monitoring. This research utilized the MOD13A2.061 Terra Vegetation Indices 16-Day Global 1 km dataset to extract NDVI data, specifically employing the NDVI band with 1 km spatial resolution and over 23 satellite image scenes from the years 2013, 2019, and 2022. A time series analysis was performed for the province of Ankara. The MOD13A2.061 dataset was brought in as a set of images (Rakuasa et al., 2023). We used the area of interest, Ankara, and the time period of interest, 2013–2022, to narrow down the image collection. The NDVI band was chosen from the collection of filtered images (Chen et al., 2025). We calculated the average NDVI for each pixel over the selected time period. We did a time series analysis on the NDVI.

In Fig. 4., the normalized difference vegetation index (NDVI) goes from -1 to 1. Negative values indicate less vegetation in areas that aren't vegetated (Rahimi et al., 2025). From 2013 to 2022, the NDVI value decreased slightly due to increased land development. The NDVI ranges from -0.10 to 0.75 each year. The northern part of the map shows that there are forests and other vegetation areas where the NDVI value is higher. The NDVI value increases in the summer, possibly due to the presence of more green space. The NDVI value is lower in cities than it is in the countryside. NDVI is higher in places where the plantations are healthy (Sohail et al., 2023). It was found that NDVI was higher in the summer because of the greenery, and it was lower in cities than in rural areas.

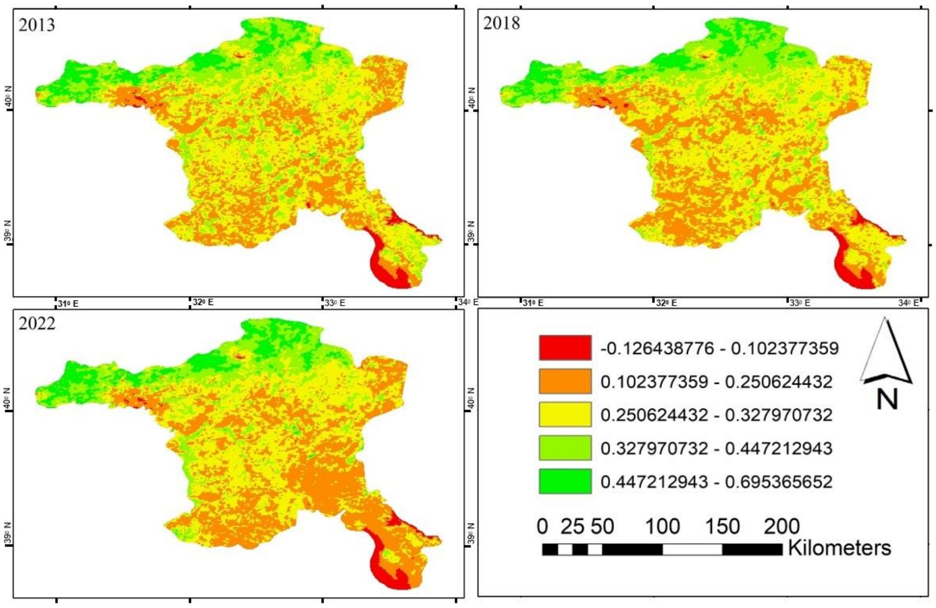

Fig. 4. 2013–2022 Map showing the NDVI pattern between
Source: own compilation

In Fig. 5., This graph shows how NDVI values changed from 2013 to 2022, making it easy to see how they changed from season to season and year to year. In the spring and summer, values are especially high.

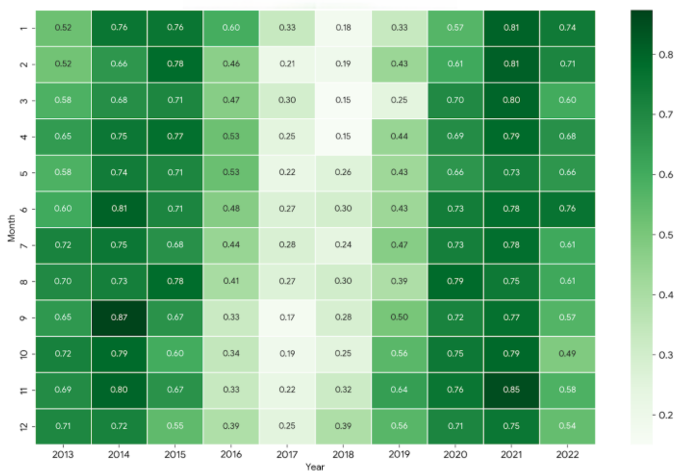

Fig. 5. NDVI Time Series (2013–2022)
Source: own compilation

In Fig. 6., High NDVI values indicated a significant amount of forest or vegetation. The MOD13A2.061 dataset provided NDVI data over 16 days, enabling time-series analysis to detect changes in vegetation cover and health at that frequency (Gaikwad & Israr, 2025). Nonetheless, it is crucial to acknowledge that the integrity of NDVI data may be influenced by factors such as cloud cover, meteorological conditions, and the existence of snow or water (Sohail et al., 2023). So, it's important to use the right filtering and quality control methods to make sure the analysis is correct.

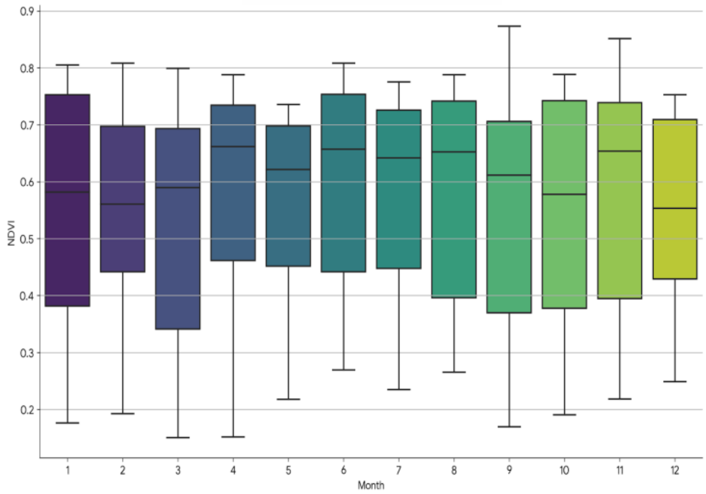

Fig. 6. Ankara Monthly Average NDVI Values
Source: own compilation

NDBI monitoring. To compute and assess NDBI, GEE provides an array of tools for image processing, data visualization, and analysis (Zhang et al., 2025). GEE also has access to a large library of satellite images that can be used to study NDBI at different times and places (Gadekar et al., 2023). We used the MOD09A1.061 Terra Surface Reflectance 8-Day Global 500m data for the sur_refl_b02 (near-infrared) and sur_refl_b06 (shortwave infrared) bands to figure out the Normalized Reconstruction Index (NDBI). ArcGIS Pro remote sensing software (Guha et al., 2021) was used to process the MOD09A1.061 Terra Surface Reflectance 8-Day Global 500m data. The study's scope and the data subset were delineated to encompass the province of Ankara for the years 2013, 2019, and 2022. Using Equation (3), we found the NDBI for each scene.

$$\mathrm{NDBI} = \frac{(\mathrm{sur\_refl\_b06} - \mathrm{sur\_refl\_b02})}{(\mathrm{sur\_refl\_b06} + \mathrm{sur\_refl\_b02})} \tag{3}$$

Normalized by rescaling the NDBI values to the range 0 to 1 using formula (4).

$$\mathrm{NDBI}_{\mathrm{normalized}} = \frac{(\mathrm{NDBI} - min_{\ NDBI})}{(max_{\ NDBI} - min_{\ NDBI})} \tag{4}$$

In Fig. 7., a graph and map were used to show the NDBI time series, which showed changes in space and time in residential areas (Gadekar et al., 2023).

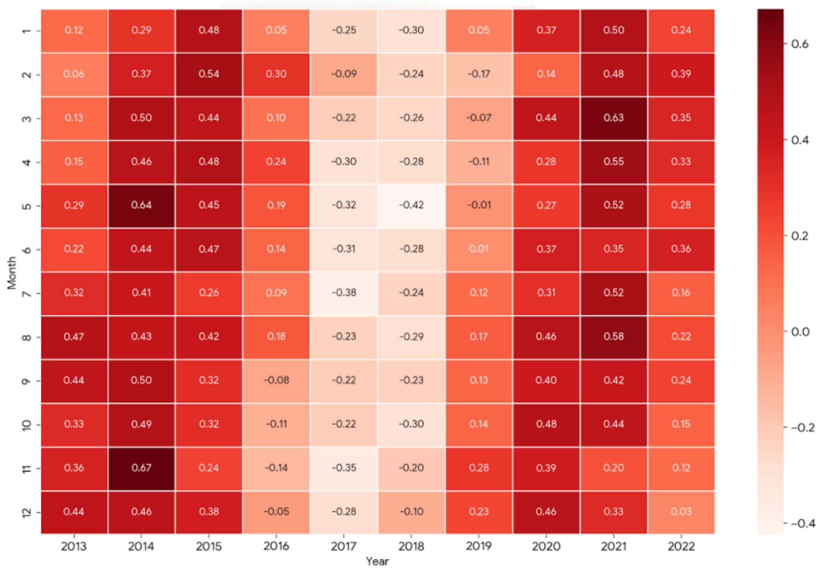

Fig. 7. Ankara NDBI Time Series (2013–2022)
Source: own compilation

NDBI is like NDVI in that it shows the normalized difference between built-up areas. The value can be anywhere from -1 to 1. A positive NDBI value means that there are more buildings and less vegetation (Guha et al., 2021). Compared to natural areas like grass or water, buildings and pavements reflect more short-wave infrared (SWIR) light and less green light. In 2013, there was slightly less built-up land than in 2022. Maps show that NDBI values are higher near cities and around farms.

In Fig. 8 and Fig. 9., the northeastern part will have the lowest NDBI value in 2022 because it has less developed forested areas. From 2013 to 2022, the population grew, leading to an increase in the number of buildings. When determining the NDBI, bodies of water were not overlooked. This might explain why the average NDBI values are negative. Excluding water bodies is expected to lead to better results in the NDBI calculation.

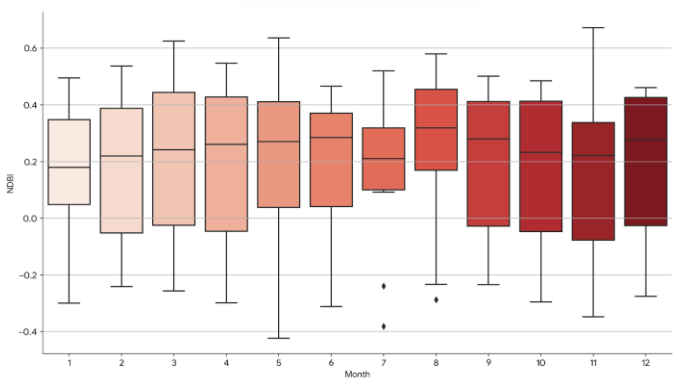

Fig. 8. Ankara Annual Average NDBI (2013–2022)
Source: own compilation

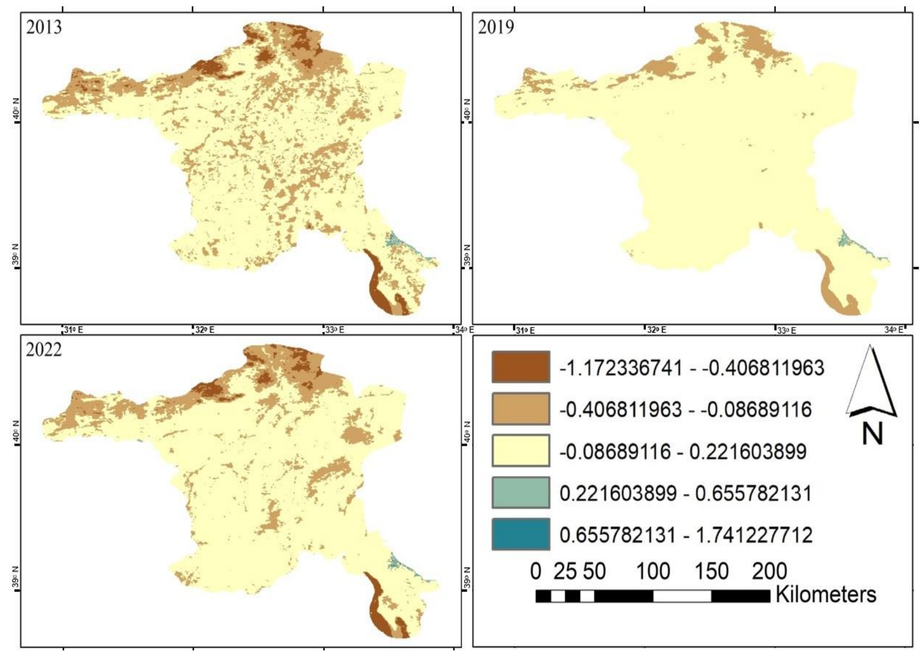

Fig. 9. 2013–2022 Map showing the NDBI pattern between
Source: own compilation

Relationship between Land Surface Temperature and NDVI and NDBI. The vegetation index, or NDVI, measures the difference in reflectance between the near-infrared and red bands (Chatterjee et al., 2025). Because plants tend to absorb more visible light and reflect more near-infrared radiation, they can be used as a stand-in for vegetation cover. According to Sohail et al. (2023), low NDVI values mean that the vegetation is sparse, while high NDVI values mean that the vegetation is dense. Thermal sensors on satellites and other remote sensing devices measure the Earth's surface temperature, which is called LST (Anand et al., 2025). It can be used to learn more about the urban heat island effect, among other things. Scatterplots of NDVI, NDBI, and LST are a useful way to look at the link between vegetation cover and temperature. You can look at how vegetation and temperature are related by making scatterplots of NDVI, NDBI, and LST measurements. In places with more plants, the temperature tends to be lower. This shows that NDVI, NDBI, and LST are positively correlated. On the other hand, a negative correlation means the opposite. Using scatter plots, you can find any outliers or strange data points that could be caused by measurement errors, cloud contamination, or other things (Makaya et al., 2025). So, scatter plots were used to show the relationship between LST and NDVI-NDBI for these projects.

In Fig 10., the northeastern part will have the lowest NDBI value in 2022 because it has less developed forested areas. From 2013 to 2022, the population grew, leading to an increase in the number of buildings. When determining the NDBI, bodies of water were not overlooked. This might explain why the average NDBI values are negative. Excluding water bodies is expected to lead to better results in the NDBI calculation.

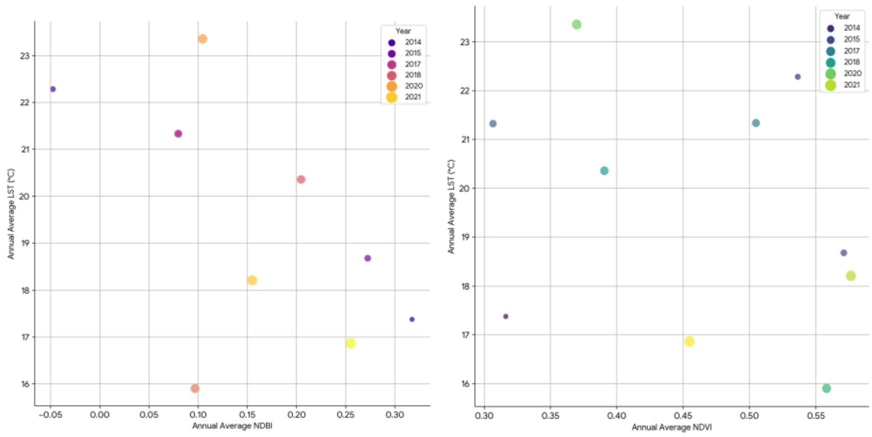

Fig. 10. Annual Average LST and NDVI-NDBI Relationship in Ankara (2013–2022)
Source: own compilation

The study's methods were used to figure out the yearly NDVI, NDBI, and LST values for each year from 2013 to 2022. Then, an Excel file was created with a scatter plot, using LST on the y-axis and NDBI on the x-axis. In the scatter plot, each point of data represents a specific time and place. By examining the scatter plot for trends or patterns, we can see how NDVI-NDBI and LST are related. When NDVI-NDBI and LST are positively correlated, it means that developed areas tend to be warmer than undeveloped areas. When they are negatively correlated, it means the opposite. By using other types of analysis, such as regression or correlation analysis, to determine the strength and nature of the relationship between NDVI-NDBI and LST, we can gain a deeper understanding of the factors contributing to urban heat island effects. This information can be useful for urban planning and environmental management.

The correlation analysis conducted in the study quantitatively elucidates the relationship between variables. The correlation matrix showed that NDVI and LST had a strong positive correlation of 0.84. There was also a positive correlation of 0.74 between LST and NDBI. There was, however, a negative correlation of -0.5 between Year and NDBI and -0.21 between Year and LST (Fig. 11).

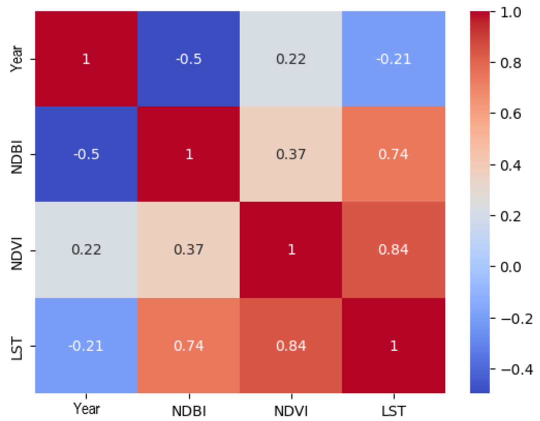

Fig. 11. Correlation diagram between variables
Source: own compilation

In Fig. 11., the northeastern part will have the lowest NDBI value in 2022 because it has less developed forested areas. From 2013 to 2022, the population grew, leading to an increase in the number of buildings. When determining the NDBI, bodies of water were not overlooked. This might explain why the average NDBI values are negative. Excluding water bodies is expected to lead to better results in the NDBI calculation.

These findings demonstrate that NDVI and LST are not negatively correlated, as previously assumed, but are instead positively correlated. This can be seen as making the surface temperature rise in the study area where there is more vegetation. This illustrates how factors such as intensive farming, the greenhouse effect, or the type of surface cover can impact various aspects.

The graphs demonstrate that LST exhibits a weaker (negative) correlation with NDVI. When LST increased, NDVI decreased slightly. On the y-axis, you can see NDVI values, and on the x-axis, you can see LST values. The slope of the distribution line is steeper in rural areas than in urban areas. This means that LST is dropping quickly in rural areas while NDVI is rising. This information can help people make decisions about planning land use, protecting the environment, and designing cities to make them more sustainable and resilient. In cities, the negative correlation between LST and NDVI is weaker than in rural areas. The negative correlation was less strong in rural areas than in urban areas. The trend line shows that LST and NDVI are not as closely related as they used to be.

Discussion

There was a change in the spatial and temporal pattern of LST for Ankara. The annual average value of LST was higher in summer than in winter. Sheik Mujabar (2019) found that LST was higher in the summer than in the winter and that it ranged from 40 to 50 °C in cities. Examining the LST pattern for each year from 2013 to 2022 revealed that LST decreased in some years instead of increasing. This could be because of other weather changes caused by global warming. Also, LST was found in cities instead of the countryside. It would be possible to do a similar analysis for places with more people living close together.

The fact that NDVI values are decreasing in cities, especially near city centers, indicates that cities have a significant impact on the amount of vegetation cover. The seasonal changes in NDVI, with higher values in the summer, could be because there is more vegetation cover at that time of year. This study also shows that there are similarities in the relationship between LST and NDVI in areas that don't have any vegetation, like high-density urban surfaces, wetlands, and bare soil. To sum up, LST, NDVI, and NDBI are all related to each other in a complicated way that changes depending on the type of land cover, the season, and the urban-rural gradient.

The urban-rural analysis of LST from 2013 to 2022 revealed that LST peaked in 2022, decreasing from urban to rural areas. Estoque et al. (2017) and Kumar et al. (2021) demonstrated that LST progressively diminished in rural areas in contrast to three urban centers. But LST was low near cities, and it started to go up as you got farther away from the main city. The trend of LST decreasing as you move farther away from the city is similar to this study, but there are notable differences near cities. Sarif et al. (2020) examined the LST pattern across the urban-rural interface in Kathmandu Valley and determined that LST was markedly greater than in the adjacent areas. Renc et al. (2022) discovered that water bodies exhibited low land surface temperature (LST), whereas the highest values were observed in land covers, specifically commercial and industrial zones within the continuous urban fabric.

Conclusions

Cities usually have higher LST than nearby rural areas. This is because more people live in cities, which results in fewer plants. As cities and populations grow quickly, LST will rise in these areas. We need to make plans and take steps to lessen these effects. Adding more green spaces and plantations to urban structures can help urban planners lessen this effect. This will not only cool and shade people, but it will also help buildings and pavements absorb less heat. Urban planners can utilize user-friendly tools to examine how different development scenarios impact LST. Planners can quickly determine how different planning choices impact LST in cities using these tools. This lets them make smart choices that lessen these effects. Urban planners can make cities more livable and sustainable by adding more green space and planting trees and shrubs. They can also use practical analysis tools to do this.

Funding

This research did not receive any specific grant from funding agencies in the public, commercial, or not-for-profit sectors. The authors declare that no external financial support was received for the conduct of this study, the preparation of the manuscript, data collection and analysis, interpretation of results, writing of the report, or the decision to submit the article for publication.

Declaration of Competing Interests

The authors declare that they have no known competing financial interests or personal relationships that could have appeared to influence the work reported in this paper. The work was not sponsored by any organization.

Use of Generative AI and AI-Assisted Technologies

Generative AI tools were used only for language editing and grammar improvementduring the preparation of this manuscript. The authors reviewed and approved all final content.

References

Amani M.J., Tanzadeh R., Moghadas Nejad F., Kabiri Nasrabad M.M., Chalabii J., Movahedi Rad M. (2025). Urban Sustainability Through Pavement Technologies: Reducing Urban Heat Islands with Cool Pavements. Buildings, 15(3), 504.

Anand V., Kaur S., Rajput V.D., Minkina T., Mandzhieva S., Kumar S., Kumar S. (2025). Analyzing the spatial relationship between land surface temperature and normalized difference vegetation index using remote sensing and GIS. Discover Geoscience, 3(1), 65.

Ayanlade A., Aigbiremolen M.I., Oladosu O.R. (2021). Variations in urban land surface temperature intensity over four cities in different ecological zones. Scientific Reports, 11(1), 20537. https://doi.org/10.1038/s41598-021-99693-z.

Bag A., Sharma A., Pal S. (2024). Studying urbanization pattern in Sambalpur City during 1992–2042 using CA-ANN, and Markov-Chain model. International Journal of Engineering and Geosciences, 9(3), 356–367.

Basu J., Sarkar G., Sarkar R., Mukhopadhyay A., Sikdar P.K. (2025). Current Status of Climate Vulnerability in Kolkata Urban Agglomeration in the Context of Proposed Resilience and Adaptation. In India III: Climate Change and Landscape Issues in India: A Cross-Disciplinary Framework (pp. 407–443). Cham: Springer Nature Switzerland.

Cao L., Li P., Zhang L. (2008). Impact of impervious surface on urban heat island in Wuhan, China. In International conference on earth observation data processing and analysis. ICEODPA. vol. 7285, pp. 1690–1698. SPIE.

Chatterjee S., Baath G.S., Sapkota B.R., Flynn K.C., Smith D.R. (2025). Enhancing LAI estimation using multispectral imagery and machine learning: A comparison between reflectance-based and vegetation indices-based approaches. Computers and Electronics in Agriculture, 230, 109790.

Chen R., Xiong S., Zhang N., Fan Z., Qi N., Fan Y., Cheng J. (2025). Fine-scale classification of horticultural crops using Sentinel-2 time-series images in Linyi country, China. Computers and Electronics in Agriculture, 236, 110425.

Didan K. (2015). MOD13A2 MODIS/Terra Vegetation Indices 16-Day L3 Global 1km SIN Grid V006 [Data set]. NASA EOSDIS Land Processes DAAC. https://doi.org/10.5067/MODIS/MOD13A2.006.

Dissanayake D. (2020). Land Use Change and Its Impacts on Land Surface Temperature in Galle City, Sri Lanka. Climate, 8(5), 65. https://doi.org/10.3390/cli8050065.

Estoque R.C., Murayama Y., Myint S.W. (2017). Effects of landscape composition and pattern on land surface temperature: An urban heat island study in the megacities of Southeast Asia. Science of The Total Environment, 577, 349–359. https://doi.org/10.1016/j.scitotenv.2016.10.195.

ESRI (2024). ArcGIS Pro (Version 3.2) [Computer software]. Environmental Systems Research Institute. https://www.esri.com/en-us/arcgis/products/arcgis-pro/ [access: 30.03.2026].

Gadekar K., Pande C.B., Rajesh J., Gorantiwar S.D., Atre A.A. (2023). Estimation of land surface temperature and urban heat island by using google earth engine and remote sensing data. In Climate Change Impacts on Natural Resources, Ecosystems and Agricultural Systems, pp. 367–389. Cham: Springer International Publishing.

Gaikwad S., Israr M. (2025). Vegetation condition monitoring and analysis using time series satellite dataset. SPAST Reports, 2(1).

Guha S., Govil H., Gill N., Dey A. (2021). A long-term seasonal analysis on the relationship between LST and NDBI using Landsat data. Quaternary International, 575, 249–258.

Gorelick N., Hancher M., Dixon M., Ilyushchenko S., Thau D., Moore R. (2017). Google Earth Engine: Planetary-scale geospatial analysis for everyone. Remote Sensing of Environment, 202, 18–27. https://doi.org/10.1016/j.rse.2017.06.031.

Golder J., Das, J., Bhandari G. (2025). Impact of Climate Change and Anthropogenic Activities on Shallow Landslide Initiation in Pangthang, East Sikkim: A Geospatial Technology and FAHP-Based Approach. Journal of The Institution of Engineers (India): Series A, 1–21.

IPCC (2021). Climate Change 2021: The Physical Science Basis. Intergovernmental Panel on Climate Change. https://www.ipcc.ch/report/ar6/wg1/ [access: 30.03.2026].

Islam A., Shirowzhan S., Pettit C.J. (2025). Geographic Information System Based Site Selection for NSW's Renewable Energy Zones: Addressing SDG 7. Sustainability, 17(6), 2708.

Karakavak H.N., Kadılar G.Ö. (2025). Benford's Law and Generalized Extreme Value Distribution in Detecting Anomalies in Air Pollution Levels: An Example from Ankara Province. Süleyman Demirel University Journal of the Institute of Science, 29(1), 176–188.

Kumar A., Agarwal V., Pal L., Chandniha D., Mishra V. (2021). Effect of Land Surface Temperature on Urban Heat Island in Varanasi City, India. J2, 4. https://doi.org/10.3390/j4030032.

Li X., Zhou W., Ouyang Z. (2013). Relationship between land surface temperature and spatial pattern of greenspace: What are the effects of spatial resolution? Landscape and Urban Planning, 114, 1–8. https://doi.org/10.1016/j.landurbplan.2013.02.005

Makaya N.V.L., Ndiaye M.L., Traore V.B., Thiam O.N. (2025). Land Use/Land Cover Dynamics Effects on Urban Heat Islands: A Case Study of Dakar Region. American Journal of Environmental Protection, 13(1), 16–30.

Mwangi P.W., Karanja F.N., Kamau P.K. (2018). Analysis of the Relationship between Land Surface Temperature and Vegetation and Built-Up Indices in Upper-Hill, Nairobi. Journal of Geoscience and Environment Protection, 06(01), 1–16. https://doi.org/10.4236/gep.2018.61001

NOAA (2023). Climate Change: Global Temperature. National Oceanic and Atmospheric Administration. https://www.climate.gov [access: 30.03.2026].

Pleniou M., Koutsias N. (2025). The role of spectral vs spatial resolution of satellite data on the accuracy of mapping unburned vegetation within fire scar perimeters. Science of Remote Sensing, 100241.

Qian W., Rao F., Li X., Lai D. (2025). Mapping priority zones for urban heat mitigation in Shanghai: Heat risk vs. shelter provision. Computers, Environment and Urban Systems, 121, 102330.

Rahimi E., Dong P., Jung C. (2025). Global NDVI-LST correlation: Temporal and Spatial patterns from 2000 to 2024. Environments, 12(2), 67.

Rahman H.U., Ding H., Wang G., Ullah S., Khan A. (2025). Impacts of Spatio-temporal land use land cover changes on the Development of Urban Heat Islands in a Diverse Topographic Region of District Nowshera, Pakistan. International Journal of Engineering and Geosciences, 11(2), 363–374.

Rakuasa H., Sihasale D.A., Latue P.C. (2023). Spatial pattern of changes in land surface temperature of seram island based on google earth engine cloud computing. International Journal of Basic and Applied Science, 12(1), 1–9.

Ravanelli R., Nascetti A., Cirigliano R., Di Rico C., Leuzzi G., Monti P., Crespi M. (2018). Monitoring the Impact of Land Cover Change on Surface Urban Heat Island through Google Earth Engine: Proposal of a Global Methodology, First Applications and Problems. Remote Sensing, 10(9), 1488. https://doi.org/10.3390/rs10091488.

Renc A., Łupikasza E., Błaszczyk M. (2022). Spatial structure of the surface heat and cold islands in summer based on Landsat 8 imagery in southern Poland. Ecological Indicators, 142, 109181. https://doi.org/10.1016/j.ecolind.2022.109181.

Sarif Md. O., Rimal B., Stork N.E. (2020). Assessment of Changes in Land Use/Land Cover and Land Surface Temperatures and Their Impact on Surface Urban Heat Island Phenomena in the Kathmandu Valley (1988–2018). ISPRS International Journal of Geo-Information, 9(12), 726. https://doi.org/10.3390/ijgi9120726.

Sari D.N., Rianti D.I., Sukmahati S.M., Rini A.M. P. (2024). Monitoring Spatio-Temporal of Vegetation Indices Using NDVI and EVI Algorithms on Google Earth Engine (GEE) in Tuntang Watershed Area, Indonesia. In IOP Conference Series: Earth and Environmental Science, vol. 1406, no. 1, p. 012026. IOP Publishing.

Sattar T., Mirza N.F., Javed M.A., Nasar-u-Minallah M., Malik S. (2025). Changing pattern of urban landscape and its impact on thermal environment of Lahore; Implications for climate change and sustainable development. Environmental Monitoring and Assessment, 197(2), 151.

Saxena V. (2025). Water quality, air pollution, and climate change: investigating the environmental impacts of industrialization and urbanization. Water, Air, Soil Pollution, 236(2), 73.

Sheik Mujabar P. (2019). Spatial-temporal variation of land surface temperature of Jubail Industrial City, Saudi Arabia due to seasonal effect by using Thermal Infrared Remote Sensor (TIRS) satellite data. Journal of African Earth Sciences, 155, 54–63. https://doi.org/10.1016/j.jafrearsci.2019.03.008.

Shi H., Xian G. (2025). Assessing gap-filled Landsat land surface temperature time-series data using different observational datasets. International Journal of Remote Sensing, 1–24.

Sohail M.T., Manzoor Z., Ehsan M., Al-Ansari N., Khan M.B., Shafi A., Ullah J., Hussain A., Raza D., Usman U., Akbar S., Elbeltagi A. (2023). Impacts of urbanization, LULC, LST, and NDVI changes on the static water table with possible solutions and water policy discussions: A case from Islamabad, Pakistan. Frontiers in Environmental Science, 11. https://www.frontiersin.org/articles/10.3389/fenvs.2023.1018500.

Sonet M.S., Hasan M.Y., Kafy A.A., Shobnom N. (2025). Spatiotemporal analysis of urban expansion, land use dynamics, and thermal characteristics in a rapidly growing megacity using remote sensing and machine learning techniques. Theoretical and Applied Climatology, 156(2), 79.

Sür İ. B., Algancı U., Sertel E. (2025). Evaluating the performance of deep learning-based segmentation algorithms for land use land cover mapping in a heterogenous vegetative environment. International Journal of Engineering and Geosciences, 10(3), 380–397.

TSI (2023). Address-Based Population Registration System Results. Turkish Statistical Institute. https://www.tuik.gov.tr [access: 30.03.2026].

TSI (2024). Address-Based Population Registration System Results. Turkish Statistical Institute. https://www.tuik.gov.tr [access: 30.03.2026].

Ullah S., Khan M., Qiao X. (2025). Evaluating the impact of urbanization patterns on LST and UHI effect in Afghanistan's Cities: a machine learning approach for sustainable urban planning. Environment, Development and Sustainability, 1–42.

UN-Habitat (2020). World Cities Report 2020: The Value of Sustainable Urbanization. United Nations Human Settlements Programme. https://unhabitat.org [access: 30.03.2026].

Vermote E. (2015). MOD09A1 MODIS/Terra Surface Reflectance 8-Day L3 Global 500m SIN Grid V006 [Data set]. NASA EOSDIS Land Processes DAAC. https://doi.org/10.5067/MODIS/MOD09A1.006.

Wan Z., Hook S., Hulley, G. (2015). MOD11A2 MODIS/Terra Land Surface Temperature/Emissivity 8-Day L3 Global 1km SIN Grid V006 [Data set]. NASA EOSDIS Land Processes DAAC. https://doi.org/10.5067/MODIS/MOD11A2.006.

Wang Z.-H., Upreti R. (2019). A scenario analysis of thermal environmental changes induced by urban growth in Colorado River Basin, USA. Landscape and Urban Planning, 181, 125–138. https://doi.org/10.1016/j.landurbplan.2018.10.002.

Zhang J., Zou B., Yuan Y., Khan A., Junaid M.B., Abbas Q., Alzahrani H. (2025). Three Decades of Land Cover Dynamics in a Boreal Coastal Basin: A Multi-Sensor Spectral Index and Machine Learning Approach Using Landsat Data and GB-SAR Data. IEEE Journal of Selected Topics in Applied Earth Observations and Remote Sensing.